ASN NEURO RESEARCH ARTICLE

Diverse inflammatory responses in transgenic mouse models of Alzheimer's disease and the effect of immunotherapy on these responses

Donna M Wilcock*[1], Qun Zhao*, Dave Morgan[†], Marcia N Gordon[†], Angela Everhart*, Joan G Wilson*, Jennifer E Lee* and Carol A Colton*[2]

*Division of Neurology, Duke University Medical Center, Durham, NC 27710, U.S.A.
[†]Department of Molecular Pharmacology and Physiology, USF Health Byrd Alzheimer's Institute, University of South Florida, Tampa, FL 33616, U.S.A.

ABSTRACT

While the presence of an inflammatory response in AD (Alzheimer's disease) is well known, the data on inflammation are conflicting, suggesting that inflammation either attenuates pathology, exacerbates it or has no effect. Our goal was to more fully characterize the inflammatory response in APP (amyloid precursor protein) transgenic mice with and without disease progression. In addition, we have examined how anti-Aβ (amyloid β-peptide) immunotherapy alters this inflammatory response. We have used quantitative RT–PCR (reverse transcription–PCR) and protein analysis to measure inflammatory responses ranging from pro-inflammatory to anti-inflammatory and repair factors in transgenic mice that develop amyloid deposits only (APPSw) and amyloid deposits with progression to tau pathology and neuron loss [APPSw/NOS2$^{-/-}$ (nitric oxide synthase 2$^{-/-}$)]. We also examined tissues from previously published immunotherapy studies. These studies were a passive immunization study in APPSw mice and an active vaccination study in APPSw/NOS2$^{-/-}$ mice. Both studies have already been shown to lower amyloid load and improve cognition. We have found that amyloid deposition is associated with high expression of alternative activation and acquired deactivation genes and low expression of pro-inflammatory genes, whereas disease progression is associated with a mixed phenotype including increased levels of some classical activation factors. Immunotherapy targeting amyloid deposition in both mouse models resulted in decreased alternative inflammatory markers and, in the case of passive immunization, a transient increase in pro-inflammatory markers. Our results suggest that an alternative immune response favours retention of amyloid deposits in the brain, and switching away from this state by immunotherapy permits removal of amyloid.

Key words: alternative activation, amyloid deposition, immunotherapy, microglia, neuroinflammation.

INTRODUCTION

AD (Alzheimer's disease) is defined pathologically by the presence of amyloid plaques composed of aggregated Aβs (amyloid β-peptides) and NFTs (neurofibrillary tangles) composed of hyperphosphorylated and aggregated tau protein. These primary AD pathologies are associated with 'activated' microglia and reactive astrocytes. It was this initial observation of activated inflammatory cells surrounding the amyloid plaques and NFTs that stimulated the interest in the role of inflammation in AD. Subsequent studies demonstrated numerous pro-inflammatory immune factors in autopsied brains of humans diagnosed with AD (McGeer et al., 1987; Walker et al., 2001; Lue and Walker, 2002; Rogers et al., 2007). Despite the body of data showing inflammation in AD, the precise changes in inflammatory state and the impact of such changes throughout the progression of AD are unknown.

In the periphery, the inflammatory responses to stimuli are much better understood than the brain. For instance, there are variety of responses ranging from a true pro-inflammatory response, termed classical inflammation, through to repair and anti-inflammatory responses, termed alternative inflammation (Martinez et al., 2009). Classical inflammation is characterized by high expression of IL-1β (interleukin 1β), TNFα (tumour necrosis factor α) and IL-6 and occurs following an acute stimulus such as a stab wound, an acute infection or the acute phase of an ischaemic attack. Alternative inflammation is characterized by high levels of AG1 (arginase 1), IL-1 receptor antagonist, MR (mannose receptor) and IL-4. Finally, a third major inflammatory state has been described that is associated with an active down-regulation of inflammation, termed acquired deactivation. This state is characterized by high levels of TGFβ (transforming growth factor β), SPHK1 (sphingosine kinase 1) and CD163 (reviewed by Colton, 2009). Although well characterized in the periphery, it is unclear whether the brain is capable of the full spectrum of the above-described inflammatory responses. The goal of the current study was to determine how inflammatory responses are both driven by, and directly influence, amyloid deposition with and without progression to tau pathology and neurodegeneration.

We have examined the expression of specific classical inflammation, alternative inflammation and acquired deactivation genes and, where possible, their proteins, in mouse models of AD that show amyloid deposition only (APPSw) and amyloid deposition accompanied by tau hyperphosphorylation and aggregation and neuronal loss [APPSw/NOS2$^{-/-}$ (nitric oxide synthase 2$^{-/-}$)]. In addition, we have examined brain tissues from previously published anti-Aβ immunotherapy studies to determine how this therapeutic approach alters the basal inflammatory state of the brain (Wilcock et al., 2004a, 2009). Our results show that, first, the brain is capable of generating a spectrum of inflammatory responses much like those found in the periphery. Secondly, our results suggest that amyloid deposition alone is primarily associated with alternative inflammation. However, when there is disease progression to tau pathology and neuro-degeneration, there is expression of classical inflammatory genes and acquired deactivation, as well as those for alternative inflammation. Finally, immunotherapy results in a significant decrease in expression of alternative inflammation genes, along with a transient increase in classical inflammation genes. These gene changes occur prior to the observation of significant amyloid reductions, suggesting that inflammation may have a causal role in the pathogenesis of AD, or at least in the progression of amyloid pathology.

MATERIALS AND METHODS

Animals

The APPSw/NOS2$^{-/-}$ mouse strain was generated as described previously (Colton et al., 2006b) and aged until 52–60 weeks before use in the experiments on assessment of inflammatory status. APPSw and NOS2$^{-/-}$ mice (B6 129P2NOS2^{tau1Lau}/J; Jackson Labs) (Laubach et al., 1998) of the same age were used as littermate controls. APPSw mice were also studied at 12 and 106 weeks of age. Animals were fed standard mouse chow and housed under 12 h light/12 h dark cycles at 21°C in an approved barrier facility. The number of mice analysed ranged from six to ten mice per data point and groups were composed of approximately equal males and females.

Tissue processing/immunocytochemistry

All mice used in these studies were killed using a lethal dose of anaesthesia using a mixture of ketamine/xylazine prior to harvest of tissue according to Duke University IACUC approved procedures and National Institutes of Health guidelines on animal care. Maximum care was taken to minimize the number of mice used and to alleviate any suffering. Mice were killed followed by intracardial perfusion with 25 ml of normal PBS. Brains were rapidly removed and bisected in the mid-sagittal plane. One-half of the brain was immersion fixed in 4% PFA (paraformaldehyde), while the other was snap-frozen in liquid nitrogen and stored at −80°C (for genotype studies and for the active vaccination study), or dissected, frozen on solid CO_2 and stored at −80°C (for the passive immunization study). Fixed tissue was processed and 25 μm sections were collected as described previously (Wilcock et al., 2004b, 2009). Free-floating immunohistochemistry was used to detect the regional localization of MR. The percentage area occupied by Aβ-positive immunostain was measured as described previously (Wilcock et al., 2004a).

Quantitative real-time RT–PCR (reverse transcription–PCR)

RNA was extracted from the frozen tissue using the PerfectPure RNA tissue kit (5 Prime Inc.) and, subsequently, cDNA produced using the high-capacity cDNA archive kit (Applied Biosystems). Real-time PCR was performed using the TaqMan Gene Expression assay kit (Applied Biosystems) according to the manufacturer's instructions and as previously described (Colton et al., 2006a). The genes examined are shown in Table 1 and were normalized to 18S rRNA. Normal WT (wild-type) mice served as the comparator and fold changes were calculated using the $2^{(-\Delta\Delta Ct)}$ method (Livak and Schmittgen, 2001).

Western–blot analysis

Protein was extracted from pulverized brain powder and quantified using the BCA (bicinchoninic acid) protein assay kit (Thermo Scientific), according to manufacturer's instructions. Proteins (15 μg) from each lysate were run on a denaturing SDS/ 4–20% PAGE gel. The gel was transferred on to a PVDF membrane, and Western-blot analyses were performed for AG1 [Santa Cruz Biotechnology (catalogue no. sc-20150); 1:1000, stains

Table 1   **Identification of gene probes used in the experiments**

Mouse gene	Ref Seq
Arg1/AG1	NM_007482
CD163	NM_053094
CAT2 (SLC7A2)	NM_007514
Chi3l3 (YM1)	NM_009892
IL1rn	NM_031167
IL-1β	NM_008361
MARCO	NM_010766
Mrc1	Nm_008625
Nos2	NM_010927
Sphk2	NM_203280
TGFβ	NM_011577
HO-1	NM_010442
IL-6	NM_031168
TNFα	NM_013693

multiple bands in the 37–45 kDa range], TGFβ [Cell Signaling Technology (catalogue no. 3711); 1:1000, stains multiple bands in the 25–45 kDa range] or β-actin [Santa Cruz Biotechnology (catalogue no. sc-1616); 1:1000]. The blots were stripped using Restore stripping buffer (Thermo Scientific) and re-probed using the above protocol with β-actin as loading control. Semi-quantitative densitometry analysis was performed using the FluorChem Q (Cell BioSciences). Individual densitometry values were normalized to the β-actin densitometry value from the same sample.

Statistics
The significance of genotype- and treatment-specific changes was analysed by the unpaired Student's *t* test or ANOVA using JMP 9 (SAS) or GraphPad Prism 4 (GraphPad).

Anti-Aβ immunotherapy
Brain samples were taken from mice that had previously undergone active vaccination with either human Aβ-(1–42) peptide or KLH (keyhole-limpet haemocyanin). All mice used in the active vaccination study were aged 12 months and then vaccinated four times over a 4-month period. Mice were killed at 16 months of age. Amyloid loads and cognition data from this vaccination study were published previously (Wilcock et al., 2009) and are summarized in Table 2.

We also re-used brain samples from a passive immunization study. In this case previously harvested, frozen hippocampi were taken from passively immunized APPSw (Tg2576) mice. This study was previously published with respect to the effects on amyloid load and cognition (Wilcock et al., 2004a), and these results are also summarized in Table 2. Here, 19-month-old APPSw mice were assigned to one of the four groups, control antibody for 3 months or anti-Aβ antibody 2286 [antibody 2286, mouse monoclonal anti-human Aβ-(28–40) IgG1; Rinat Neuroscience Corporation] at a dose of 10 mg/kg intraperitoneal for 1 month, 2 months or 3 months (*n*=4 mice/group). The start of treatment was staggered such that all mice were killed at the same age. In this manner, a time course of changes with passive immunization was generated. Age-matched control APPSw mice were injected intraperitoneal with mouse monoclonal anti-*Drosophila*

amnesiac protein (AMN) IgG1 antibody (Rinat Neuroscience Corporation) at a dose of 10 mg/kg for 3 months. In all cases, tissue processing in vaccinated mice was the same as described above for mice used in the inflammatory status experiments.

RESULTS

Mice with only amyloid pathology show an alternative inflammatory response, while those with disease progression show mixed alternative and classical
Using quantitative real-time RT–PCR, we examined the differences in gene expression profiles between WT and NOS2$^{-/-}$ control mice that show no disease pathology, and mice that show either amyloid deposition only (APPSw; Tg2576), or amyloid deposition plus disease progression to tau pathology and neuronal loss (APPSw/NOS2$^{-/-}$). Analysis of the brain pathology of the mice used in the study has been previously published and described in detail (Colton et al., 2006b; Wilcock et al., 2009) and results are summarized in Table 2. Figure 1 shows the relative change in mRNA for classical inflammatory markers (*IL-1β, TNFα, IL-6, MARCO* and *CAT2*), alternative inflammatory markers (*YM1, AG1* and *IL1rn*) and acquired deactivation markers (*TGFβ, SphK* and *HO-1*) for our transgenic mice using age-matched WT mice as the reference group. As previously shown, NOS2$^{-/-}$ mice kept under barrier conditions do not deviate from WT levels of inflammatory gene expression (Colton et al., 2006a). In contrast, the APPSw mice at 12 months, an age when there is amyloid pathology present in the brain, demonstrate inflammatory changes. In APPSw mice, we found little to no expression of pro-inflammatory genes (Figure 1A). The most notable classical inflammatory changes were small but statistically significant increases in *IL-1β, MARCO* and *CAT2* mRNA levels. In contrast, gene expression levels for markers of immunosuppressive states (*YM1, AG1, IL-1rn, TGFβ* and *Sphk1*) were significantly increased compared with WT and NOS2$^{-/-}$ mice (Figure 1B). To determine whether the lack of pro-inflammatory

Table 2 Summary of previously published data for mouse pathology and anti-Aβ immunotherapy studies
Numbers in brackets are the number of mice. *$P<0.05$ compared with APPSw; CAA, cerebral amyloid angiopathy (vascular amyloid); RAWM, radial arm water maze.

Study	Mouse model	Age (months)	Histopathological data				Cognition	References
			Total Aβ (pg/ml)	CAA	p-tau soma	Neuron loss		
Non-treated	APPSw	12–16	662 ± 100 (5)	+	None	None	Decrease Y maze; increase latency to platform [Morris water maze]; no change from NOS2$^{-/-}$ (RAWM)	(Hsiao et al., 1996; Colton et al., 2006b; Wilcock et al., 2008, 2009)
Non-treated	APPSw/NOS2$^{-/-}$	12–16	3172 ± 1072* (3)	+++	++	Down ~30%	Decrease (RAWM)	(Colton et al., 2006b; Wilcock and Colton, 2008; Wilcock et al., 2009)
Passive immunization	APPSw	19–22	Decrease 60%	Increase 4-fold	n/a	n/a	Improved	(Wilcock et al., 2004a; 2004b)
Active vaccination	APPSw/NOS2$^{-/-}$	12–16	Decrease 85%	No change	Down 50–60%	No further loss	Reversed	(Wilcock et al., 2009)

markers was due to the age of the APPSw mice, we also measured mRNA changes for *IL6*, *TNFα*, *IL-1b*, *CAT2* and *MARCO* in 12- and 106-week-old control APPSw mice. No significant statistical changes in mRNA levels were found in any inflammatory marker in 12-week-old mice, but *TNFα* and *HO-1* mRNA were slightly but significantly raised in 106-week-old mice (see Supplementary Figure S1 available at http://www.asnneuro.org/an/003/an003e069add.htm).

APPSw/NOS2$^{-/-}$ mice at 12 months show amyloid pathology, tau hyperphosphorylation, aggregation and redistribution to neuronal soma as well as significant neuronal loss, therefore representing a model of amyloid deposition with disease progression (Colton et al., 2006b; Wilcock and Colton, 2008; Wilcock et al., 2009). These APPSw/NOS2$^{-/-}$ mice showed a shift in the immune phenotype from a predominately alternative inflammation in the APPSw alone to a mixed inflammatory state expressing both classical inflammation and alternative inflammation. Classical inflammatory genes (*IL-6*, *IL-1β* and *CAT2*) significantly increased compared with APPSw, NOS2$^{-/-}$ or WT control mice. Expression of alternative inflammation and acquired deactivation genes such as *YM1* and *AG1* was significantly lower in the APPSw/NOS2$^{-/-}$ compared with APPSw mice, yet still elevated compared with NOS2$^{-/-}$ and WT mice. In contrast, expression of *IL-1rn*, *SphK* and *HO-1* increased, while expression of *TGFβ* remained at the same elevated level observed in the APPSw mice. A mixed inflammatory state is consistent with chronic inflammatory disease (Wynn, 2008) and is also seen in brains of humans with AD (Colton et al., 2006a).

To determine whether protein levels were changed in a manner consistent with the observed changes in mRNA, we performed ELISAs and Western blottings where reliable antibodies were available. ELISA assays were performed for TNFα and IL-6 on brain lysates from each of the mice used in the study. As shown in Figure 2, the protein levels of IL-6 (Figure 2A) and TNFα (Figure 2B) were either unchanged or slightly increased in APPSw mice compared with WT and NOS2$^{-/-}$ mice. However, in APPSw/NOS2$^{-/-}$ mice, both cytokines were significantly increased. TNFα protein levels increased approximately 200%, while IL-6 protein levels were increased by approximately 80% over the values observed in WT, NOS2$^{-/-}$ or APPSw mice. Semi-quantitative Western blottings from whole brain lysates were used to measure protein expression for AG1 and TGFβ, characteristic proteins for alternative inflammation and acquired deactivation respectively. Typical blots for each of these proteins with their corresponding density measurements are shown in Figure 3 and show similar patterns of changes as found in the corresponding mRNA levels. AG1 levels were significantly increased in APPSw but not in APPSw/NOS2$^{-/-}$ mice compared with WT, while TGFβ levels in both APPSw and APPSw/NOS2$^{-/-}$ were increased compared with WT mice. The increased TGFβ levels were not significantly different between APPSw and APPSw/NOS2$^{-/-}$ mice.

To this point, all data have been obtained on RNA and protein extracts from whole-brain samples. We were
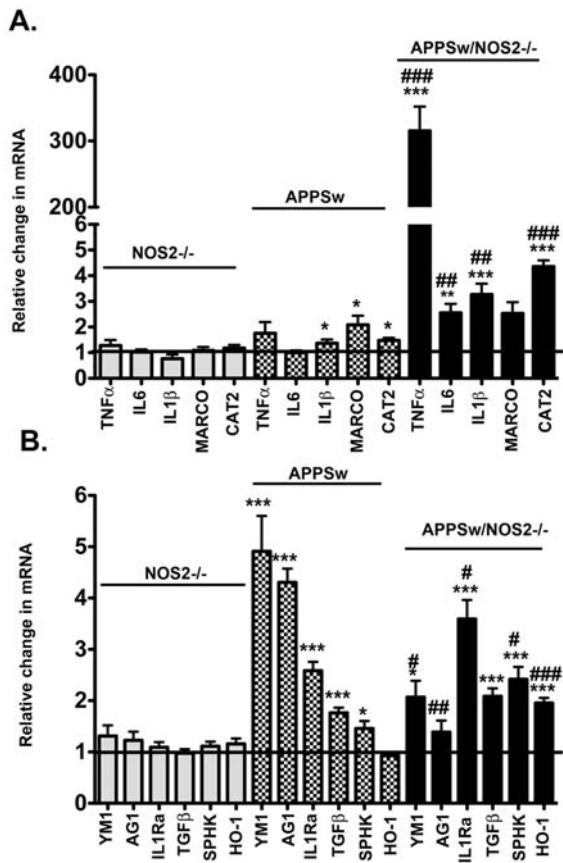
Figure 1 Comparison of mRNA expression levels for classical activation, alternative activation and acquired deactivation genes associated with the brain's innate immune response between a mouse model of amyloid deposition and a model of disease progression

Results represent the means $\pm$ S.E.M. fold-change in mRNA levels for classical activation genes (**A**) and for alternative activation genes and acquired deactivation genes (**B**) in 52–60-week-old NOS2$^{-/-}$, APPSw and APPSw/NOS2$^{-/-}$ mice brain samples compared with WT control mice of the same age (n=5–7 mice per strain). *P<0.05, **P<0.01, ***P<0.001 compared with the NOS2$^{-/-}$ control mice in each case. #P<0.05, ##P<0.01, ###P<0.001 compared with the parent strain.

Figure 2 Average protein levels for TNFα and IL–6
Means$\pm$S.E.M. protein levels in whole brain lysates from 52–60-week-old WT, NOS2$^{-/-}$, APPSw and APPSw/NOS2$^{-/-}$ mice were measured using standard ELISA assays (n=5–7 mice per strain). *P<0.05, ***P<0.001 compared with the NOS2$^{-/-}$ or WT control mice. ###P<0.001 compared with the parent strain.

interested in determining, where possible, potential regional contributions to the overall gene expression profiles. To achieve this, we measured gene expression for two genes that are known to be localized to perivascular microglia, that is, *Mrc1* (mannose receptor C1 gene) and *CD163* (Hb-haptoglobin scavenger receptor gene) (Fabriek et al., 2005; Galea et al., 2005; Borda et al., 2008; Hawkes and McLaurin, 2009). Figure 4(A) shows the relative changes in mRNA prepared from whole-brain samples for these genes in each of the mouse strains used in the study. *Mrc1* was significantly increased in APPSw and in APPSw/NOS2$^{-/-}$ mice compared with WT and NOS2$^{-/-}$, with no difference between APP (amyloid precursor protein) models. CD163 was significantly increased only in the APPSw/NOS2$^{-/-}$ compared with the WT, NOS2$^{-/-}$ and APPSw. To determine whether changes in MR protein expression could be observed in the perivascular compartment, we performed immunohistochemistry on brain
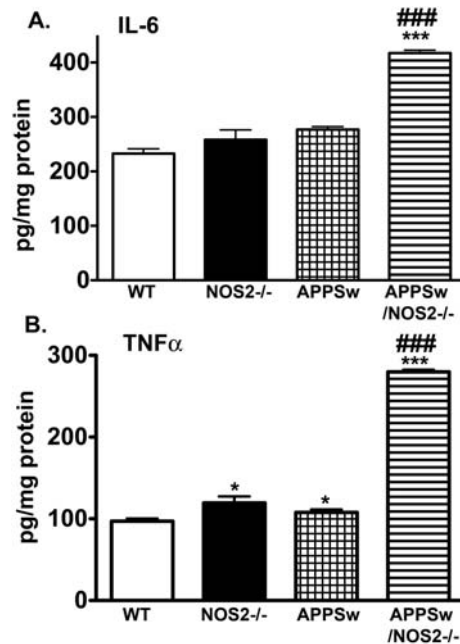
sections from WT, NOS2$^{-/-}$, APPSw and APPSw/NOS2$^{-/-}$ mice aged 12 months. MR positive staining was localized to the cerebrovasculature and resembled staining patterns previously observed by Hawkes and McLaurin (2009). MR-positive cells were localized throughout the brain in all sections examined (subiculum is shown as an example, Figures 4B–4D). Interestingly, fine cellular processes were also stained in the subiculum of the APPSw/NOS2$^{-/-}$ mice, in addition to the intense staining around the cerebral blood vessels, giving a 'fuzzy' appearance (Figure 4D). We did not observe such staining in the APPSw or control mice.

Anti–Aβ immunotherapy results in a shift in the inflammatory state

Passive immunization is an approach in which monoclonal antibodies are directly administered. We have examined gene expression changes in a previously published passive immunization study that showed the time course of Aβ reductions (Table 2 summarizes previously published data). Briefly, APPSw mice received weekly immunizations of anti-Aβ antibody for 1, 2 or 3 months with the start age staggered such that all mice were killed at 22 months of age. As shown in the previously published data for this study, Aβ levels remained high after 1 month of treatment, but significantly decreased after 2 and 3 months of treatment. These changes are illustrated in Figure 5(A). To determine the effect that immunotherapy has on the inflammatory state, we measured
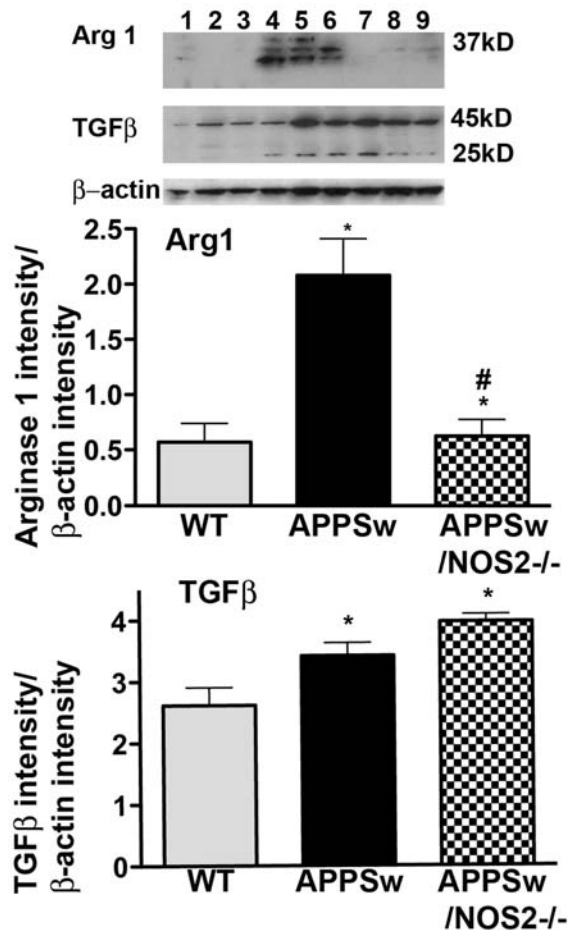
Figure 3 Western–blot analysis of AG1 and TGFβ protein levels
Western blottings were performed using whole-brain lysates and the relative band density of each antigen compared with β-actin was calculated for AG1 and for TGFβ. All band intensities were measured using the FluorChem Q (Cell Biosciences). Lanes 1–3, WT; lanes 4–6, APPSw; lanes 7–9, APPSw/NOS2$^{-/-}$; *$P < 0.05$ compared with the WT$^{-/-}$ control mice; $^\#P < 0.05$ compared with the parent strain.

A similar analysis was performed for mice that had undergone active vaccination where mice develop anti-Aβ antibodies as a result of immunogen injection, in this case, vaccination with Aβ42. We have previously published the results of this active vaccination study with respect to changes in Aβ, tau, neuronal loss and cognition, and these data are also summarized in Table 2. Briefly, we vaccinated 12-month-old APPSw/NOS2$^{-/-}$ mice four times over a 4-month period, which resulted in an 85% reduction in brain Aβ deposition, as well as the prevention of neuron loss and a 50% decrease in phospho-tau levels. We have now examined gene expression changes associated with classical inflammation, alternative inflammation and acquired deactivation in samples of these mice brains. Vaccinated APPSw/NOS2$^{-/-}$ mice showed significant reductions in *TNFα* and *IL-6* mRNA compared with control vaccinated APPSw/NOS2$^{-/-}$ mice, yet *TNFα* and *IL-6* mRNAs were still significantly increased compared with WT and NOS2$^{-/-}$ mice (Figure 6A). Interestingly, alternative inflammatory genes *YM1* and *AG1* were significantly reduced, not only compared with control vaccinated APPSw/NOS2$^{-/-}$ but also compared with WT and NOS2$^{-/-}$ mice (Figure 6B). In addition, *TGF*β was reduced approximately to WT levels following vaccination (Figure 6B). Inflammatory genes *Mrc1* and *CD163*, known to be restricted to the cerebrovasculature, decreased compared with both control vaccinated APPSw/NOS2$^{-/-}$ mice, and WT mice (Figure 6C).

DISCUSSION

Although inflammation has long been considered as an important factor in the neurodegenerative process (Schwab and McGeer, 2008; Rivest, 2009; Cameron and Landreth, 2010; Glass et al., 2010) the exact role of inflammation in neurodegeneration is not yet fully understood. A commonly held view is that amyloid deposition results in an inflammatory response that generates a toxic state leading to neuronal damage and death and, ultimately, contributing to the progression of degeneration. Much of the supporting data for this hypothesis has originated from studies using *in vitro* cultured cells or brain slices, or *in vivo* modelling of acute inflammatory responses using agents such as LPS (lipopolysaccharide) (Klegeris et al., 1994; Hu et al., 1995; Meda et al., 1999; Colton et al., 2000; Lee et al., 2002; Block and Hong, 2005; Bernardino et al., 2008). While acute approaches have been useful, the disparate data that have resulted from these types of studies have been difficult to resolve (Abbas et al., 2002; Quinn et al., 2003; Malm et al., 2006; Shaftel et al., 2007; Nichol et al., 2008). These data can be explained somewhat by variations in experimental design, mouse models and even differences in background strains of mice. However, there is a clear need for a better understanding of the relationship between inflammatory state and neurodegenerative processes. In the present study, we have

gene expression changes in the hippocampus for classical inflammation (Figure 5B), alternative inflammation and acquired deactivation (Figure 5C). Interestingly, significant changes in the inflammatory state occurred prior to any change in Aβ levels. Following 1 month of treatment, classical inflammatory genes *IL-6* and *TNFα* were significantly increased compared with APPSw mice receiving control immunotherapy (Figure 5B). In contrast, 1 month after the treatment, alternative inflammatory genes *YM1* and *AG1*, normally high in APPSw mice, were significantly reduced compared with APPSw mice receiving control immunotherapy (Figure 5C). The most dramatic change was in *AG1*, where the expression actually decreased significantly compared with WT mice. The acquired deactivation genes *Sphk1* and *TGF*β were significantly increased after 1 month of treatment and continued to increase over the 2- and 3-month treatment periods (Figure 5C). While most gene changes remained for the 2- and 3-month treatment periods, *IL-6* mRNA levels declined in comparison with the 1 month time point (Figure 5B).
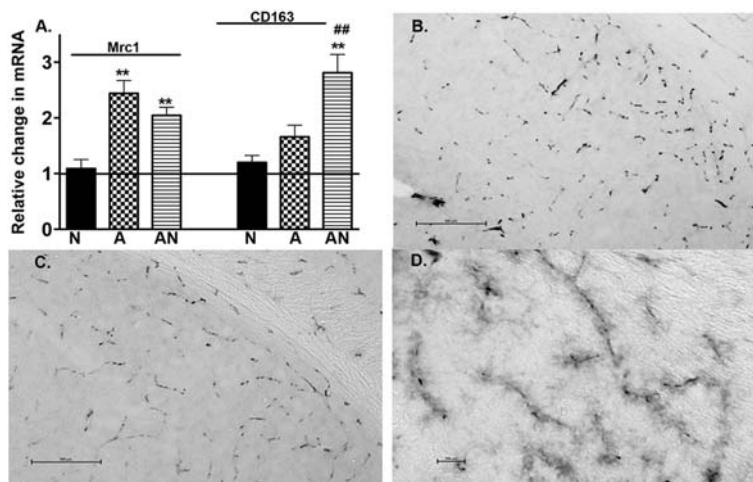
Figure 4   Changes in expression for MR and CD163
(**A**) The average relative change in mRNA was determined using quantitative RT–PCR for MR (*Mrc1*) and the hemoglobin-haptaglobin scavenger receptor (*CD163*) for NOS2$^{-/-}$ (N), APPSw (**A**) and APPSw/NOS2$^{-/-}$ (AN) mice ($n=$5–7 mice per strain). **$P<$0.01 compared with the NOS2$^{-/-}$ control. ##$P<$0.01 compared with the parent strain. (**B–D**) Immunostained sections for MR in NOS2$^{-/-}$ (**B**; magnification $\times$20; scale bar=500 µm) and in APPSw/NOS2$^{-/-}$ mice at low (**C**; magnification $\times$20; scale bar=500 µm) and at higher magnification (**D**; $\times$40; scale bar=100 µm).

examined a broad spectrum of inflammatory markers that represent three different inflammatory states: classical inflammation, alternative inflammation and acquired deactivation. Each of these states have been shown, both in the periphery and in the CNS (central nervous system), to have very different consequences to disease process. We had several goals for this study. The first goal was to better establish markers for each inflammatory state and determine their expression in the brain. The second goal was to determine how these states are expressed in a mouse model of amyloid deposition (APPSw) and a mouse model of amyloid deposition with disease progression to tau pathology and neuron loss (APPSw/NOS2$^{-/-}$). Finally, our third goal was to determine how anti-Aβ immunotherapy, an approach currently in clinical trials for the treatment of AD and is known to reduce Aβ levels in the brain, affects the inflammatory state.

We have examined markers of three distinct inflammatory states (Gordon, 2003; Ransohoff and Perry, 2009; Perry et al., 2010). Classical inflammation is characterized by increased expression of *TNFα*, *IL-1β* and *IL-6* and is commonly associated with a pro-inflammatory, cellular toxicity response. However, it is important to note that these markers can be also increased in response to immune complexes or other induction signals, and do not necessarily lead to toxicity. Alternative inflammation is characterized by high expression levels of the genes *YM1*, *AG1*, *Mrc1* and *IL-1rn* and is stimulated by anti-inflammatory factors such as IL-4 and IL-13. While many of these genes are considered 'repair' genes involved in matrix restructuring and tissue repair, as well as the down-regulation of the classical inflammatory response, their effects may not be fully beneficial. Finally, acquired deactivation is characterized by high *TGF*β, *Sphk1* and *HO-1* gene expression levels. This

inflammatory state can be directly stimulated by glucocorticoids or apoptotic cells, is immunosuppressive and actively lowers the ability to mount a classical inflammatory response (Ransohoff and Perry, 2009; Cameron and Landreth, 2010; Colton and Wilcock, 2010).

Our data show that amyloid deposition, in the absence of tau pathology and neuronal loss, results in a polarization to alternative inflammation and acquired deactivation, as opposed to the classical inflammation that is commonly considered to be present. This polarization in the APPSw mouse model is characterized by high expression levels of alternative inflammation mRNA for *YM1*, *AG1* and *IL-1rn*, which were anywhere from 2.5- to more than 5-fold increased compared with WT and NOS2$^{-/-}$ mice at 12 months of age. This time period is clearly associated with elevated Aβ40 and Aβ42 levels and amyloid deposition (Jacobsen et al., 2006). Interestingly, in 3-month-old APPSw mice where Aβ levels remain below levels of detection (Jacobsen et al., 2006), no changes in alternative activation genes were observed. In contrast, we found that classical inflammation genes *TNFα*, *IL-6* and *IL-1*β were only marginally increased in 12-month-old APPSw mice, if at all, compared with WT and NOS2$^{-/-}$ mice. In addition, acquired deactivation genes *TGF*β, *Sphk1* and *HO-1* were also increased compared with WT and NOS2$^{-/-}$ mice. Based on the current knowledge of the function of the corresponding proteins, the brain's immune phenotype found in the APPSw mice is more likely to be associated with matrix restructuring and down-regulation of classical inflammatory signalling rather than toxicity (Gordon, 2003; Colton, 2009). It is important to point out that our data do not identify a specific cell type involved in this immune process. Although *AG1* and *YM1* and their proteins have been clearly identified in microglia, these
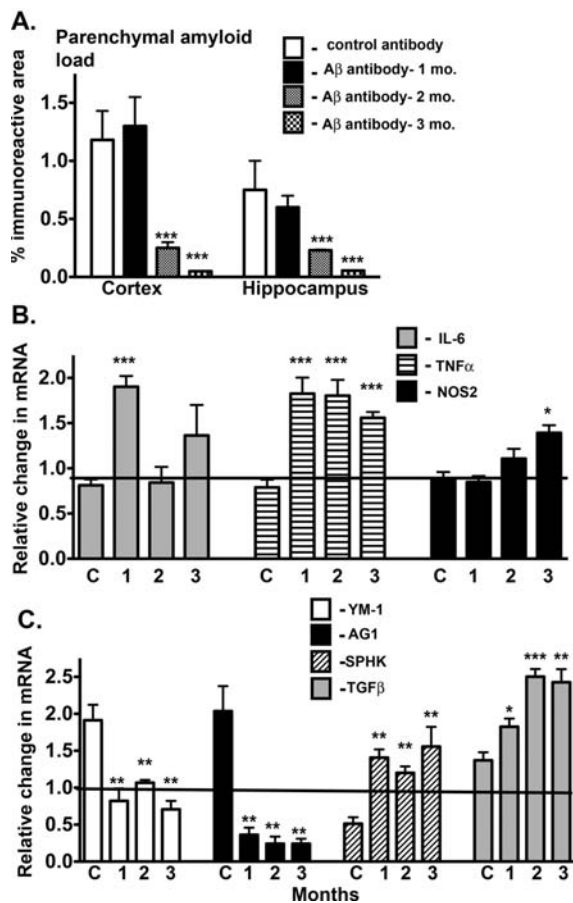
Figure 5 Passive immunization alters the immune profile in APPSw mice
(A) Parenchymal amyloid load in the cortex and hippocampus. As described in the Materials and methods section, 19-month-old APPSw mice were assigned to one of four groups, control antibody for 3 months or anti-Aβ antibody 2286 (Rinat Neurosciences) for 1, 2 or 3 months ($n=4$/group). The start of dosing was staggered such that all mice were of the same age when killed. The level of amyloid immunostain in brains from passively immunized APPSw mice was measured by image analysis of immunostained regions as described in the Materials and methods section. Results are presented as the means $\pm$ S.E.M. of the % immunoreactive area. (B, C) Results represent the means $\pm$ S.E.M. fold-change in mRNA levels for selected classical activation genes (B) and for alternative activation and acquired deactivation genes (C) in immunized compared with control mice starting at 9 months of age ($n=4$ mice/group). *$P<0.05$, **$P<0.01$, ***$P<0.001$ compared with control mice.

Figure 6 Active immunization alters the immune profile in APPSw/NOS2$^{-/-}$ mice
Mice were immunized with either Aβ-(1–42) or KLH at 12 months of age as described in the Materials and methods section and compared with age-matched NOS2$^{-/-}$ mice immunized in a similar fashion. (A, B) Results represent the means $\pm$ S.E.M. fold-change in mRNA levels for selected classical activation genes (A) and for selected alternative activation and acquired deactivation genes (B) in APPSw/NOS2$^{-/-}$ mice. (C) mRNA for alternative activation genes (Mrc1; CD163) associated with the cerebrovasculature ($n=5$–7 mice/group in all cases). **$P<0.01$, ***$P<0.001$ compared with control mice. #$P<0.05$, ##$P<0.01$ compared with the Aβ42 immunized condition in each case.

genes are also expressed by neurons and/or astrocytes (Braissant et al., 1999; Junker et al., 2005; Colton et al., 2006a; Ponomarev et al., 2007). Interestingly, Ch3L1 (chitinase-3-like-1; also known as YKL40), which is a close relative of Ch3L3 (the human equivalent of *YM1*) has been recently shown to increase in CSF (cerebrospinal fluid) in patients with early MCI (mild cognitive impairment) (Craig-Schapiro et al., 2010). Multiple factors including restricted regional expression or age may have also contributed to the immune polarization observed in the APPSw mice. To better understand the effects of age, we also measured mRNAs for inflammatory genes in 12- and 106-week-old APPsw mice. Pro-inflammatory gene expression did not change compared with littermate WT mice in young mice, while only *TNFα* and
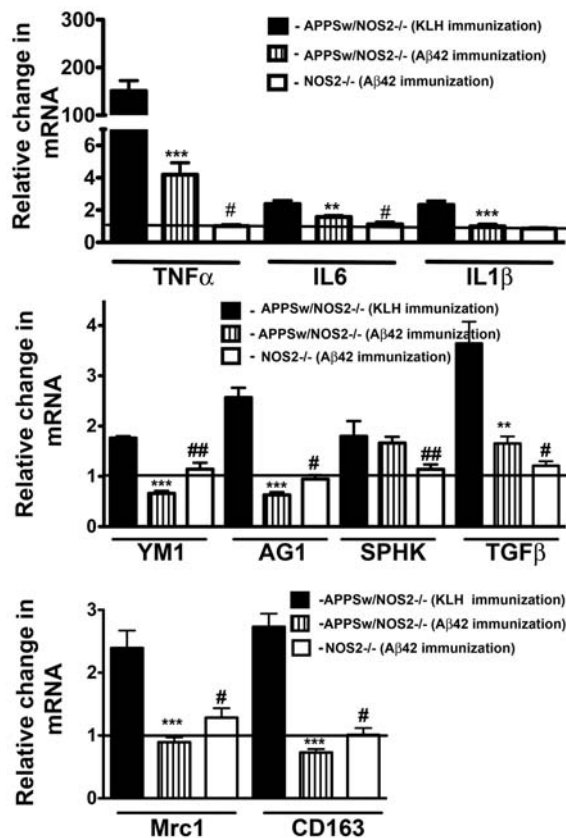
HO-1 mRNAs were slightly elevated in the very old APPSw mice. These data further support the idea that amyloid deposition in the absence of extensive disease progression may be associated with immunosuppression rather than overt toxicity.

The inflammatory profile of the APPSw/NOS2$^{-/-}$ mouse model that shows amyloid deposition with disease progression to tau pathology and neuron loss is clearly different from the profile observed in the APPSw mice alone. The main difference is that, in addition to high alternative inflammation and acquired deactivation, the APPSw/NOS2$^{-/-}$ mice now have increased expression of classical inflammation genes. Therefore these mice truly show a full spectrum of the inflammatory states. As previously published, APPSw/NOS2$^{-/-}$ mice show a 30% hippocampal neuron loss at 54 weeks of age (Wilcock et al., 2009). The presence of high classical inflammation may,

indeed, be directly or indirectly related to this neurotoxicity. Also, the increase in acquired deactivation genes in APPSw/NOS2$^{-/-}$ mice compared with the APPSw mice may be explained by the presence of these apoptotic neurons, a known initiator of the acquired deactivation response.

We were interested in the relationship between Aβ and inflammatory state. Therefore we examined brain samples from a previously published anti-Aβ immunotherapy study for changes in the inflammatory state. We found that immunotherapy, whether active vaccination or passive immunization, or whether in APPSw or APPSw/NOS2$^{-/-}$ mice, significantly reduced the expression of alternative inflammatory markers. The time course study in passively immunized APPSw mice clearly showed that the decrease in *YM1* and *AG1* preceded the fall in Aβ levels in the brain and was concomitant with an increase in classical inflammation genes, both of which occurred after only 1 month of treatment. Active vaccination in APPSw/NOS2$^{-/-}$ mice showed that classical inflammation was decreased compared with control vaccinated APPSw/NOS2$^{-/-}$ mice, but remained higher compared with WT and NOS2$^{-/-}$ mice. The classical inflammation data may appear to be contradictory between the two studies; however, there are several important points to be considered. First, APPSw mice alone do not express high levels of classical inflammation genes, thus, any increase due to immunotherapy represents a dramatic change in level. In contrast, APPSw/NOS2$^{-/-}$ mice initially have elevated classical inflammation. Our data show that although vaccination lowered mRNA levels, the final levels were still higher than that found in normal mice. However, the single most important point from this data is that these dramatic shifts in the inflammatory state correspond to significant changes in brain Aβ levels and, as shown for passive immunization, occurs prior to the reduction in Aβ. Therefore there is likely a causal relationship between inflammation and Aβ deposition.

The change in inflammatory state due to immunotherapy, and its effect in lowering Aβ, is not necessarily surprising. Several reports demonstrate that intracranial injection of LPS, an agent known to induce classical inflammation, results in the removal of brain Aβ in APP transgenic mice (Herber et al., 2007; Morgan, 2009; Chakrabarty et al., 2010). Also, we have previously shown that microglial activation is not only associated with Aβ removal following intracranial injection of anti-Aβ antibodies, but in fact facilitates this removal (Wilcock et al., 2003). One potential mechanism for such an effect is an increase in proteolytic degradation of parenchymal Aβ. Wilcock et al. (2011) have recently demonstrated that the ratio of MMP (matrix metalloprotease) to TIMP (tissue inhibitor of MMP) is altered by Aβ immunotherapy. The present study demonstrates the overall importance of the down-regulation of alternative inflammation and the up-regulation of classical inflammation in changing brain Aβ levels. Our results suggest that amyloid deposition results in a strong polarization of the inflammatory response to alternative inflammation and, to a lesser extent, acquired deactivation. When amyloid pathology is present exclusively, very little classical inflammation is present. When disease progression occurs in the APPSw/NOS2$^{-/-}$ mice to now show tau pathology and neuron loss, there is a classical inflammatory response in addition to the alternative inflammation and acquired deactivation. It is unclear at present whether the classical inflammation causes the disease progression or whether the opposite is true. Future studies will focus on these pathways to determine the exact role. Clearly, there is a beneficial role for classical inflammation; however, since anti-Aβ immunotherapy increases classical inflammation and this effect leads to the reduction of brain Aβ. In addition, this response does not necessarily result in toxicity, as no neuron loss or cognitive deficit is observed in APPSw mice that are passively immunized, including the mice examined in the current study.

REFERENCES

Abbas N, Bednar I, Mix E, Marie S, Paterson D, Ljungberg A, Morris C, Winblad B, Nordberg A, Zhu J (2002) Up-regulation of the inflammatory cytokines IFN-gamma and IL-12 and down-regulation of IL-4 in cerebral cortex regions of APP(SWE) transgenic mice. J Neuroimmunol 126:50–57.

Bernardino L, Balosso S, Ravizza T, Marchi N, Ku G, Randle JC, Malva JO, Vezzani A (2008) Inflammatory events in hippocampal slice cultures prime neuronal susceptibility to excitotoxic injury: a crucial role of P2 × 7 receptor-mediated IL-1beta release. J Neurochem 106:271–280.

Block ML, Hong JS (2005) Microglia and inflammation-mediated neurodegeneration: multiple triggers with a common mechanism. Prog Neurobiol 76:77–98.

Borda JT, Alvarez X, Mohan M, Hasegawa A, Bernardino A, Jean S, Aye P, Lackner AA (2008) CD163, a marker of perivascular macrophages, is up-regulated by microglia in simian immunodeficiency virus encephalitis after haptoglobin-hemoglobin complex stimulation and is suggestive of breakdown of the blood-brain barrier. Am J Pathol 172:725–737.

Braissant O, Gotoh T, Loup M, Mori M, Bachmann C (1999) L-arginine uptake, the citrulline-NO cycle and arginase II in the rat brain: an *in situ* hybridization study. Brain Res Mol Brain Res 70:231–241.

Cameron B, Landreth GE (2010) Inflammation, microglia, and Alzheimer's disease. Neurobiol Dis 37:503–509.

Chakrabarty P, Jansen-West K, Beccard A, Ceballos-Diaz C, Levites Y, Verbeeck C, Zubair AC, Dickson D, Golde TE, Das P (2010) Massive gliosis induced by interleukin-6 suppresses Abeta deposition *in vivo*: evidence against inflammation as a driving force for amyloid deposition. FASEB J 24:548–559.

Colton CA (2009) Heterogeneity of microglial activation in the innate immune response in the brain. J Neuroimmune Pharmacol 4:399–418.

Colton CA, Wilcock DM (2010) Assessing activation states in microglia. CNS Neurol Disord Drug Targets 9:174–191.

Colton CA, Chernyshev ON, Gilbert DL, Vitek MP (2000) Microglial contribution to oxidative stress in Alzheimer's disease. Ann NY Acad Sci 899:292–307.

Colton CA, Mott RT, Sharpe H, Xu Q, Van Nostrand WE, Vitek MP (2006a) Expression profiles for macrophage alternative activation genes in AD and in mouse models of AD. J Neuroinflammation 3:27.

Colton CA, Vitek MP, Wink DA, Xu Q, Cantillana V, Previti ML, Van Nostrand WE, Weinberg JB, Dawson H (2006b) NO synthase 2 (NOS2) deletion promotes multiple pathologies in a mouse model of Alzheimer's disease. Proc Natl Acad Sci USA 103:12867–12872.

Craig-Schapiro R, Perrin RJ, Roe CM, Xiong C, Carter D, Cairns NJ, Mintun MA, Peskind ER, Li G, Galasko DR, Clark CM, Quinn JF, D'Angelo G, Malone JP, Townsend RR, Morris JC, Fagan AM, Holtzman DM (2010) YKL-40: a novel prognostic fluid biomarker for preclinical Alzheimer's disease. Biol Psychiatry 68:903–912.

Fabriek BO, Van Haastert ES, Galea I, Polfliet MM, Dopp ED, Van Den Heuvel MM, Van Den Berg TK, De Groot CJ, Van Der Valk P, Dijkstra CD (2005) CD163-positive perivascular macrophages in the human CNS express molecules for antigen recognition and presentation. Glia 51:297–305.

Galea I, Palin K, Newman TA, Van Rooijen N, Perry VH, Boche D (2005) Mannose receptor expression specifically reveals perivascular macrophages in normal, injured, and diseased mouse brain. Glia 49:375–384.

Glass CK, Saijo K, Winner B, Marchetto MC, Gage FH (2010) Mechanisms underlying inflammation in neurodegeneration. Cell 140:918–934.

Gordon S (2003) Alternative activation of macrophages. Nat Rev Immunol 3:23–35.

Hawkes CA, McLaurin J (2009) Selective targeting of perivascular macrophages for clearance of beta-amyloid in cerebral amyloid angiopathy. Proc Natl Acad Sci U.S.A 106:1261–1266.

Herber DL, Mercer M, Roth LM, Symmonds K, Maloney J, Wilson N, Freeman MJ, Morgan D, Gordon MN (2007) Microglial activation is required for Abeta clearance after intracranial injection of lipopolysaccharide in APP transgenic mice. J Neuroimmune Pharmacol 2:222–231.

Hsiao K, Chapman P, Nilsen S, Eckman C, Harigaya Y, Younkin S, Yang F, Cole G (1996) Correlative memory deficits, Abeta elevation, and amyloid plaques in transgenic mice. Science 274:99–102.

Hu S, Sheng WS, Peterson PK, Chao CC (1995) Cytokine modulation of murine microglial cell superoxide production. Glia 13:45–50.

Jacobsen JS, Wu CC, Redwine JM, Comery TA, Arias R, Bowlby M, Martone R, Morrison JH, Pangalos MN, Reinhart PH, Bloom FE (2006) Early-onset behavioral and synaptic deficits in a mouse model of Alzheimer's disease. Proc Natl Acad Sci USA 103:5161–5166.

Junker N, Johansen JS, Hansen LT, Lund EL, Kristjansen PE (2005) Regulation of YKL-40 expression during genotoxic or microenvironmental stress in human glioblastoma cells. Cancer Sci 96:183–190.

Klegeris A, Walker DG, McGeer PL (1994) Activation of macrophages by Alzheimer beta amyloid peptide. Biochem Biophys Res Commun 199:984–991.

Laubach VE, Foley PL, Shockey KS, Tribble CG, Kron IL (1998) Protective roles of nitric oxide and testosterone in endotoxemia: evidence from NOS-2-deficient mice. Am J Physiol 275:H2211–2218.

Lee YB, Nagai A, Kim SU (2002) Cytokines, chemokines, and cytokine receptors in human microglia. J Neurosci Res 69:94–103.

Livak KJ, Schmittgen TD (2001) Analysis of relative gene expression data using real-time quantitative PCR and the $2-\triangle\triangle C_t$ method. Methods 25:402–408.

Lue LF, Walker DG (2002) Modeling Alzheimer's disease immune therapy mechanisms: interactions of human postmortem microglia with antibody-opsonized amyloid beta peptide. J Neurosci Res 70:599–610.

Malm T, Ort M, Tahtivaara L, Jukarainen N, Goldsteins G, Puolivali J, Nurmi A, Pussinen R, Ahtoniemi T, Miettinen TK, Kanninen K, Leskinen S, Vartiainen N, Yrjanheikki J, Laatikainen R, Harris-White ME, Koistinaho M, Frautschy SA, Bures J, Koistinaho J (2006) Beta-amyloid infusion results in delayed and age-dependent learning deficits without role of inflammation or beta-amyloid deposits. Proc Natl Acad Sci USA 103:8852–8857.

Martinez FO, Helming L, Gordon S (2009) Alternative activation of macrophages: an immunologic functional perspective. Annu Rev Immunol 27:451–483.

McGeer PL, Itagaki S, Tago H, McGeer EG (1987) Reactive microglia in patients with senile dementia of the Alzheimer type are positive for the histocompatibility glycoprotein HLA-DR. Neurosci Lett 79:195–200.

Meda L, Baron P, Prat E, Scarpini E, Scarlato G, Cassatella MA, Rossi F (1999) Proinflammatory profile of cytokine production by human monocytes and murine microglia stimulated with beta-amyloid[25-35]. J Neuroimmunol 93:45–52.

Morgan D (2009) The role of microglia in antibody-mediated clearance of amyloid-beta from the brain. CNS Neurol Disord Drug Targets 8:7–15.

Nichol KE, Poon WW, Parachikova AI, Cribbs DH, Glabe CG, Cotman CW (2008) Exercise alters the immune profile in Tg2576 Alzheimer mice toward a response coincident with improved cognitive performance and decreased amyloid. J Neuroinflammation 5:13.

Perry VH, Nicoll JA, Holmes C (2010) Microglia in neurodegenerative disease. Nat Rev Neurol 6:193–201.

Ponomarev ED, Maresz K, Tan Y, Dittel BN (2007) CNS-derived interleukin-4 is essential for the regulation of autoimmune inflammation and induces a state of alternative activation in microglial cells. J Neurosci 27:10714–10721.

Quinn J, Montine T, Morrow J, Woodward WR, Kulhanek D, Eckenstein F (2003) Inflammation and cerebral amyloidosis are disconnected in an animal model of Alzheimer's disease. J Neuroimmunol 137:32–41.

Ransohoff RM, Perry VH (2009) Microglial physiology: unique stimuli, specialized responses. Annual Review of Immunology 27:119–145.

Rivest S (2009) Regulation of innate immune responses in the brain. Nat Rev Immunol 9:429–439.

Rogers J, Mastroeni D, Leonard B, Joyce J, Grover A (2007) Neuroinflammation in Alzheimer's disease and Parkinson's disease: are microglia pathogenic in either disorder? Int Rev Neurobiol 82:235–246.

Schwab C, McGeer PL (2008) Inflammatory aspects of Alzheimer disease and other neurodegenerative disorders. J Alzheimers Dis 13:359–369.

Shaftel SS, Kyrkanides S, Olschowka JA, Miller JN, Johnson RE, O'Banion MK (2007) Sustained hippocampal IL-1 beta overexpression mediates chronic neuroinflammation and ameliorates Alzheimer plaque pathology. J Clin Invest 117:1595–1604.

Walker DG, Lue LF, Beach TG (2001) Gene expression profiling of amyloid beta peptide-stimulated human post-mortem brain microglia. Neurobiol Aging 22:957–966.

Wilcock DM, Colton CA (2008) Anti-amyloid-beta immunotherapy in Alzheimer's disease: relevance of transgenic mouse studies to clinical trials. J Alzheimers Dis 15:555–569.

Wilcock DM, DiCarlo G, Henderson D, Jackson J, Clarke K, Ugen KE, Gordon MN, Morgan D (2003) Intracranially administered anti-Abeta antibodies reduce beta-amyloid deposition by mechanisms both independent of and associated with microglial activation. J Neurosci 23:3745–3751.

Wilcock DM, Rojiani A, Rosenthal A, Subbarao S, Freeman MJ, Gordon MN, Morgan D (2004a) Passive immunotherapy against Abeta in aged APP-transgenic mice reverses cognitive deficits and depletes parenchymal amyloid deposits in spite of increased vascular amyloid and microhemorrhage. J Neuroinflammation 1:24.

Wilcock DM, Rojiani A, Rosenthal A, Levkowitz G, Subbarao S, Alamed J, Wilson D, Wilson N, Freeman MJ, Gordon MN, Morgan D (2004b) Passive amyloid immunotherapy clears amyloid and transiently activates microglia in a transgenic mouse model of amyloid deposition. J Neurosci 24:6144–6151.

Wilcock DM, Lewis MR, Van Nostrand WE, Davis J, Previti ML, Gharkholonarehe N, Vitek MP, Colton CA (2008) Progression of amyloid pathology to Alzheimer's disease pathology in an amyloid precursor protein transgenic mouse model by removal of nitric oxide synthase 2. J Neurosci 28:1537–1545.

Wilcock DM, Gharkholonarehe N, Van Nostrand WE, Davis J, Vitek MP, Colton CA (2009) Amyloid reduction by amyloid-beta vaccination also reduces mouse tau pathology and protects from neuron loss in two mouse models of Alzheimer's disease. J Neurosci 29:7957–7965.

Wilcock DM, Morgan D, Gordon MN, Taylor TL, Ridnour LA, Wink DA, Colton CA (2011) Activation of matrix metalloproteinases following anti-Abeta immunotherapy; implications for microhemorrhage occurrence. J Neuroinflammation 8:115.

Wynn TA (2008) Cellular and molecular mechanisms of fibrosis. J Pathol 214:199–210.